Optimization of the t/10 offset correlation method to obtain the yield strength with the Small Punch Test

Jose Calaf-Chica[(1)], Pedro Miguel Bravo Díez[(2)], Mónica Preciado Calzada[(3)], Maria-Jose Garcia-Tarrago[(4)]

E-mails: (1) Corresponding author, jcalaf@ubu.es ; (2) pmbravo@ubu.es; (3) mpreciado@ubu.es; (4) mjgtarrago@ubu.es
Postal address: Departamento de Ingeniería Civil, Universidad de Burgos, Avenida Cantabria s/n, E09006 Burgos, Spain

ABSTRACT

The Small Punch Test (SPT) was developed as an alternative test to evaluate the mechanical properties of materials from a small material volume. Although the SPT is close to its standardization as a mechanical testing method, there are many methodologies for the estimation of the different mechanical properties. All of them are based on the use of a correlation equation to link the SPT and the estimated mechanical property. The scattering of these correlation methods is generally great enough to make it necessary to delve deeper into the understanding of the physical behavior of the SPT.

This investigation was based on previous numerical studies related with the multi-dependency with more than one mechanical property of the correlation methods for the yield strength estimation. Specifically, an optimization of the t/10 offset correlation method was designed introducing the minimum slope $Slope_{min}$ of the zone III of the SPT curve in the correlation equation. This optimized t/10 offset method showed a significant reduction of the scattering between its regression surface and the material data. After completing this numerical analysis, experimental tests (tensile and SPT tests) were performed to validate the new method.

Keywords: Small Punch Test, SPT, yield strength, t/10 offset method.

Note: This research did not receive any specific grant from funding agencies in the public, commercial, or not-for-profit sectors.

1 Nomenclature and Symbols

α_i	Correlation coefficient
E	Young's modulus
σ_y	Yield strength
σ_u	Ultimate tensile strength
$\varepsilon_{max\ load}$	Strain at the maximum engineering stress
n	Strain hardening coefficient
$NRMSD$	Normalized root-mean-square deviation
P_y	Yield load
R_d	Inner radius of the lower die
RE	Relative error
R_p	Punch radius
$Slope_{min}$	Minimum slope of the zone III of the SPT curve
SPT	Small Punch Test
t	Specimen thickness

2 Introduction

The Miniaturized Disk Bend Test (MDBT), introduced by Manahan in the early 80's, was designed as an alternative characterization method to obtain the mechanical properties of irradiated steels in nuclear vessels [1,2]. The novelty of this test was its miniature geometry, making use of the small discs that were used for TEM microstructural analysis. The main advantages of this miniature disks were the less time to irradiate the specimen and the incremented number of specimens for a similar volume of material. Manahan *et al.* wanted to obtain the mechanical properties inherent to

the uniaxial tensile test, specifically the embrittlement due to the irradiation [3]. The disk thickness was equal to 0.254 mm and its diameter equal to 3.0 mm. This specimen was positioned in a cylindrical die or support and was loaded until failure by a spherical punch with radius of 0.5 mm. In 1983, Baik *et al.* designed an optimization of the MDBT [4], named as Small Punch Test (SPT), where the setup of the test and the geometry of the disk changed significantly. In this miniature test, the specimen was clamped between two dies, upper and lower, and punched until failure with a sphere of 2.5 mm in diameter. The specimen geometry was a disk with a thickness of 0.5 mm and a diameter equal or higher than 8 mm. Figure 1(a) shows an schematic view of the SPT assembly. Baik *et al.* designed a correlation method to obtain the ductile-to-brittle transition temperature using the SPT and its punch load-displacement curve (see Figure 1(b)). This curve, named as SPT curve, showed five zones, distinguished by the mechanical behavior of the specimen [5]:

(a) Zone I. Elastic bending zone of the curve.
(b) Zone II. Transition between the elastic zone and the plastic zone.
(c) Zone III. Plastic bending or plastic hardening zone.
(d) Zone IV. Softening zone due to necking and damage initiation.
(e) Zone V. Crack growth and final failure.

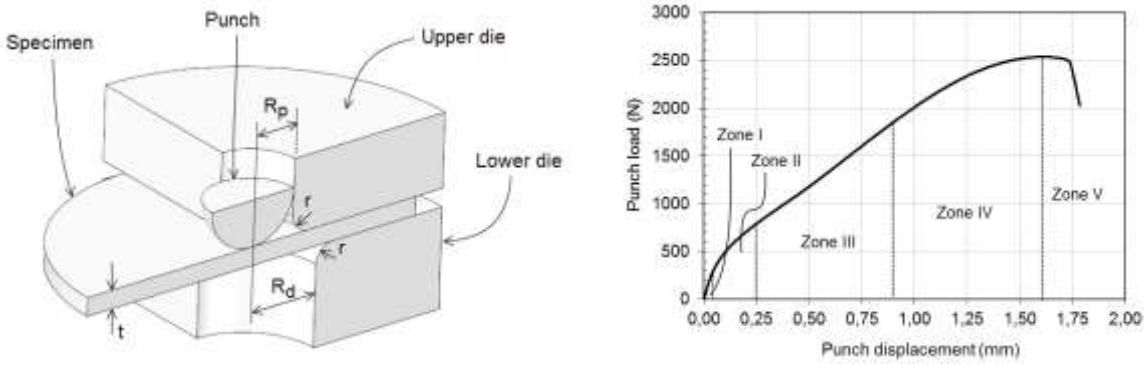

(a) (b)

Figure 1. (a) SPT set up and (b) Experimental SPT curve

After these first investigations, this miniature test has shown an exponential increase in its development, until reach the current state. The SPT is nowadays used to obtain a variety of material mechanical properties based on a small volume of material: Young's modulus [6,7], yield strength [8,9], ultimate tensile strength [10,11], ductile to brittle transition temperature [12,13], fracture properties [14,15] and creep behavior [16,17]. These mechanical properties are not directly registered with the SPT. Different parameters are obtained from the SPT curve and a correlation equation with each mechanical property must be empirically obtained. Afterwards, this correlation equation may be used to characterize similar materials with the SPT. In 2006, CEN published a guidance to the use of the SPT, identified as CWA 15627 [18], where a code of practice was established in order to initialize a standardization of this miniature test. The use of the SPT as a mechanical characterization test is limited to isotropic and homogeneous materials when the mechanical properties inherent to the uniaxial tensile test are evaluated.

The current investigation showed in this article was centered in the yield strength and how it is obtained with the SPT. Nowadays, this mechanical property has an extended variety of correlation methods. The first one, was designed by Mao *et al.* in 1987 [5], where two tangents were drawn in the zone I and III of the SPT curve (see Figure 2). The load of the crossing point between these lines, named as yield load P_y, was linearly correlated with the yield strength. Okada *et al.* [19] published an alternative correlation method based on a yield load P_y obtained with an offset line parallel to the tangent of the zone I of the SPT curve (see Figure 2). The offset was fixed to the tenth of the specimen thickness, and the yield load was obtained from the crossing point between that offset line and the SPT curve. This correlation method was named as the "t/10 offset" method. The code of practice CWA 15627 recommended a correlation method, named as CEN method, where a bilinear function was obtained minimizing an error function (see Figure 2 and equations (1) and (2)). The crossing point between the two lines which composed this bilinear function defined the yield load P_y.

$$f(u) = \begin{cases} \dfrac{f_A}{f_B}u & 0 \le u \le u_A \\ \dfrac{f_B - f_A}{u_B - u_A}(u - u_A) + f_A & u_A \le u \le u_B \end{cases} \quad (1)$$

$$err = \int_0^{u_B} [F(u) - f(u)]^2 du \quad (2)$$

where,

F(u) is the experimental SPT curve,
u is the punch displacement,
u_A is the punch displacement where the crossing point of the bilinear function is located,
u_B is the maximum punch displacement where the *err* function is calculated. The code of practice CWA 15627 recommends u_B equal to the specimen thickness,
f_A and f_B are the punch loads of points A and B.

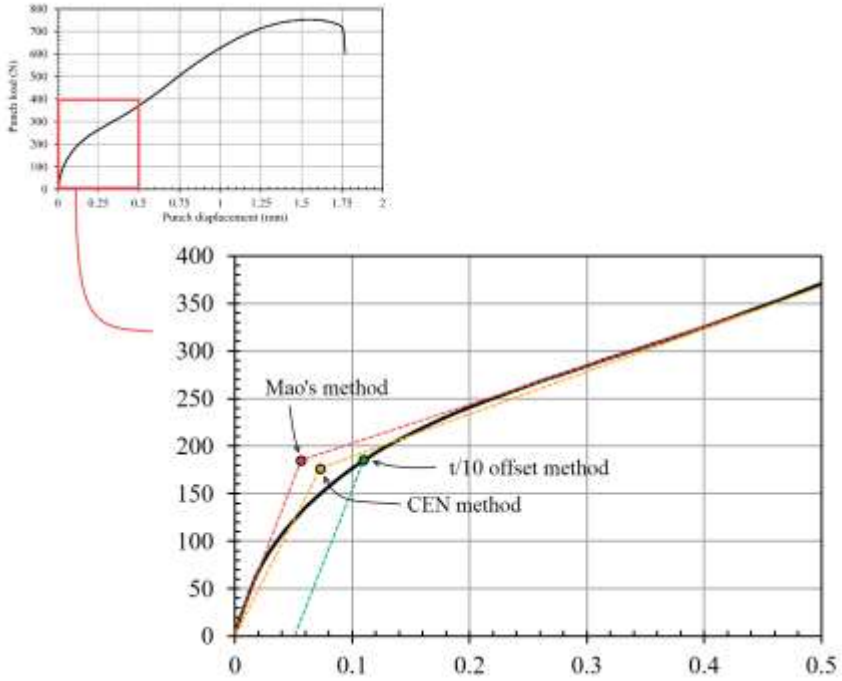

Figure 2. P_y calculation with the correlation methods for the yield strength estimation

The yield load obtained by these methods is correlated linearly with the yield strength of the material using the equation (3), where the coefficients α_1 and α_2 are obtained with a linear least squares method:

$$\sigma_y = \alpha_1 \frac{P_y}{t^2} + \alpha_2 \quad (3)$$

where:
α_1 and α_2 are correlation coefficients obtained in the linear regression,
and *t* is the specimen thickness.

The Code of Practice CWA 15627 recommends a specimen thickness t of 0.495 to 0.505 mm (0.500 mm ± 5 µm). The inherent difficulties to reach these tolerances motivated some studies of the specimen thickness influence in the SPT curve [20-21]. These studies concluded that small deviations of the thickness tolerances could be normalized factoring the punch load registered in the SPT curve with the factor $f = t_{real}^2/0.5^2$. In addition, the equation (3) included the square of the specimen thickness t in order to obtain dimensionless correlation coefficients α_i. In this investigation, all the SPT specimens were polished within the recommended tolerance to avoid the scattering generated by the application of the thickness correction factor f.

These correlation methods assumed that the yield load P_y was only or mainly dependent with the yield strength of the material, but Calaf-Chica *et al.* [22] demonstrated through a systematic FEM analysis that the coefficient α_2 was null if α_1 was considered dependent on the strain hardening of the material. In the specific case of the t/10 offset method, the obtained correlation equation (4) was dependent on an equivalent hardening coefficient n (based on the Ramberg-Osgood hardening law; see equation (5)) [23].

$$\sigma_y = \left(A_1 - \frac{1}{A_2 + A_3 \cdot n}\right) \cdot \frac{P_y}{t^2} \tag{4}$$

where,
A_1, A_2 and A_3 are the correlation coefficients to be determined in a regression analysis.

$$\varepsilon_{true} = \frac{\sigma_{true}}{E} + \varepsilon_{offset} \left(\frac{\sigma_{true}}{\sigma_y}\right)^n \tag{5}$$

where:
$\varepsilon_{offset} = 0.002$ is the plastic strain of the offset yield point,
σ_{true} is the true stress,
ε_{true} is the true strain,
E is the Young's modulus,
σ_y is the yield strength,
and n is the hardening coefficient.

Using the multi-dependent correlation equation (4), the scattering of the correlation between the yield load P_y and the yield strength diminished significantly compared with the correlation equation (3). This equation (4) was limited in use because the hardening coefficient n showed a complex rational function dependency with the SPT parameters (see equation (6)). This equation shows that n depends on the yield strength and the minimum slope of the zone III of the SPT curve ($Slope_{min}$; see Figure 3). Matching the equations (4) and (6) results in a complex equation for the calculation of the yield strength based on two values of the SPT curve: the yield load P_y, obtained from the offset t/10 method, and the minimum slope $Slope_{min}$ (see equation (7)).

$$n = \frac{B_3 \sigma_y}{Slope_{min} - \left(B_1 \sigma_y^2 + B_2 \sigma_y\right)} \tag{6}$$

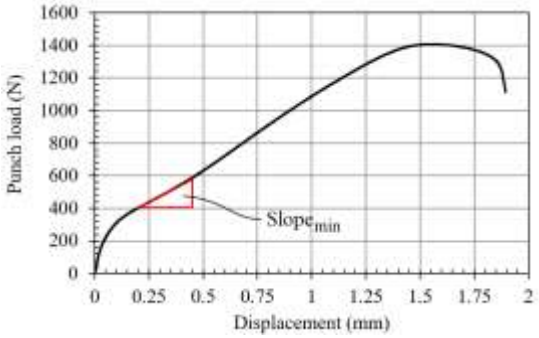

Figure 3. *Slope$_{min}$* calculation with the minimum slope method

$$\sigma_y = \left(A_1 - \frac{1}{A_2 + A_3 \left(\frac{B_3 \sigma_y}{Slope_{min} - \left(B_1 \sigma_y^2 + B_2 \sigma_y \right)} \right)} \right) \cdot \frac{P_y}{t^2} \tag{7}$$

Two facts hinder the use of this equation (7): the six correlation coefficients and the inability to get the yield strength in a simple way. Thus, one of the goals of this research was to find a way to simplify this equation (7) to obtain an optimized t/10 offset method with the use of the minimum slope *Slope$_{min}$* of the SPT curve (equation (8)).

$$\sigma_y = f\left(P_y, Slope_{min}\right) \tag{8}$$

3 Materials and Methods

As mentioned in the previous section, the aim of this investigation was to estimate the yield strength with the SPT using a regression surface dependent on the yield load P_y obtained from the t/10 offset method and the minimum slope *Slope$_{min}$* (see equation (8)).

Initially, this investigation used the database of SPT curves of a wide selection of hypothetical materials performed with the finite element method (FEM) in a previous article [22]. These were four hundred seventy-two hypothetical materials with Young's modulus ranging from 40 to 240 GPa, yield strength from 50 to 2050 MPa, and hardening coefficient *n* from 5 to 30 (based on the Ramberg-Osgood strain hardening law). Most of the metallic materials with structural purposes were covered by this database of hypothetical materials. The yield load P_y using the t/10 offset method and the minimum slope *Slope$_{min}$* were extracted from the database. The mechanical properties assigned for each hypothetical material, Young's modulus, yield strength and hardening coefficient *n*, were also used to perform the necessary correlations.

After the numerical analysis, experimental tests were developed to validate the optimized t/10 offset method. Standard tensile tests in agreement with ASTM E8M and SPTs of 16 steels were included in this analysis. Table 1 shows the mechanical properties of these steel alloys. Due to a lack of material, some alloys were tested only once. The rest of materials had three tensile test and three SPTs, calculating the mean value and the coefficient of variation. In the specific case of the DOCOL steels, they belong to a preliminary investigation [24] where different heat treatments were applied to two boron steels: DOCOL 1800 and DOCOL 2000. Details of the heat treatments are included in the previously mentioned article.

Material	***E* (GPa±%)**	**σ_y (MPa±%)**	**σ_{u_eng} (MPa±%)**	**$\varepsilon_{max\ load}$ (%±%)**
DP600	211±0.97	424±0.44	636±0.12	15.5±1.49
S275JR	205±2.34	435±1.56	478±0.10	15.9±0.80
HC260LA	203±4.67	281±0.00	374±0.13	18.9±0.92
DC06	203±1.23	125±1.13	281±0.44	25.3±2.59

S315MC	211±4.41	359±0.47	421±0.68	17.9±1.03
S420MC	208±1.85	523±0.90	593±0.44	13.5±2.08
S355MC	212±1.61	436±1.31	483±0.34	17.0±0.87
DC01	203±0.93	151±0.62	286±0.16	25.0±0.83
F1140	206±0.51	745±3.28	923±0.60	6.0±2.45
USIBOR 1500 P	209	433	599	13.0
CR-700-980-DP	207	782	1017	5.0
DOCOL 1800CR	200	807	889	2.0
DOCOL 1800 CH280	210	997	1707	6.0
DOCOL 1800 R300	211	1411	1533	3.0
DOCOL 2000 CH280	208	1027	1790	6.0
DOCOL 2000 R300	212	1421	1586	3.0

Table 1. Mechanical properties of the experimental materials

4 Numerical analyses

The parameters of the yield strength, minimum slope $Slope_{min}$ and yield load P_y of the t/10 offset method were obtained from the systematic numerical analysis of hypothetical materials [22]. Using the Curve Fitting Tool of Matlab, the coefficients A_1 to A_3 and B_1 to B_3 of the equation (7) were calculated with a non-linear least squares regression method. The deviation of this correlation was calculated with the normalized root-mean-square deviation (*NRMSD*) (see equation (9)).

$A_1 = 0.4596$
$A_2 = 1.788$
$A_3 = 1.835$
$B_1 = 2.085E\text{-}4$
$B_2 = 0.756$
$B_3 = 3.594$

$NRMSD = 12.7\%$

$$NRMSD = 100 \times \sqrt{\frac{\sum_{j=1}^{m}\sum_{i=1}^{n_j}\left[\frac{\sigma_{y_i} - \sigma_{y_j}}{\sigma_{y_j}}\right]^2}{n}} \tag{9}$$

where:
σ_{yi} is the yield strength estimated with the regression equation (7),
σ_{yj} is the yield strength pre-defined in the simulations,
n_j is the number of hypothetical materials with the same pre-defined yield strength,
m is the number of different yield strengths pre-defined in the simulations,
and n is the number of hypothetical materials ($n = \sum_{j=1}^{m} n_j$).

Figure 4 shows the regression surface (blue mesh) obtained with equation (7) and the location of hypothetical materials as red points. It is remarkable that the regression surface is nearly flat in the region where the hypothetical materials are located. Considering that the mechanical properties of the hypothetical materials were ranged to cover most of the structural metals, equation (7) could be simplified to the equation of a plane. Using the Curve Fitting Tool, the equation of the best fitted plane to the hypothetical materials, Equation (10), was obtained with the non-linear least squares regression method. Figure 5 shows the resulting regression plane (continuous straight lines), and the regression surface obtained with equation (7) (dashed lines) in the region where the hypothetical materials are located (colored circles). Both surfaces show significant overlap with the hypothetical materials. Figure 6 shows the relative error (RE) of the yield strength estimation for each hypothetical material using both equations (7) (blue bars) and (10) (orange bars). The normalized root-mean-square deviation (*NRMSD*) for the regression with the plane was 15.5% and 12.7% for the

blue surface. Thus, the simplification of equation (7) to the equation (10) generated a small increment in the regression deviation (from 12.7% to 15.5%).

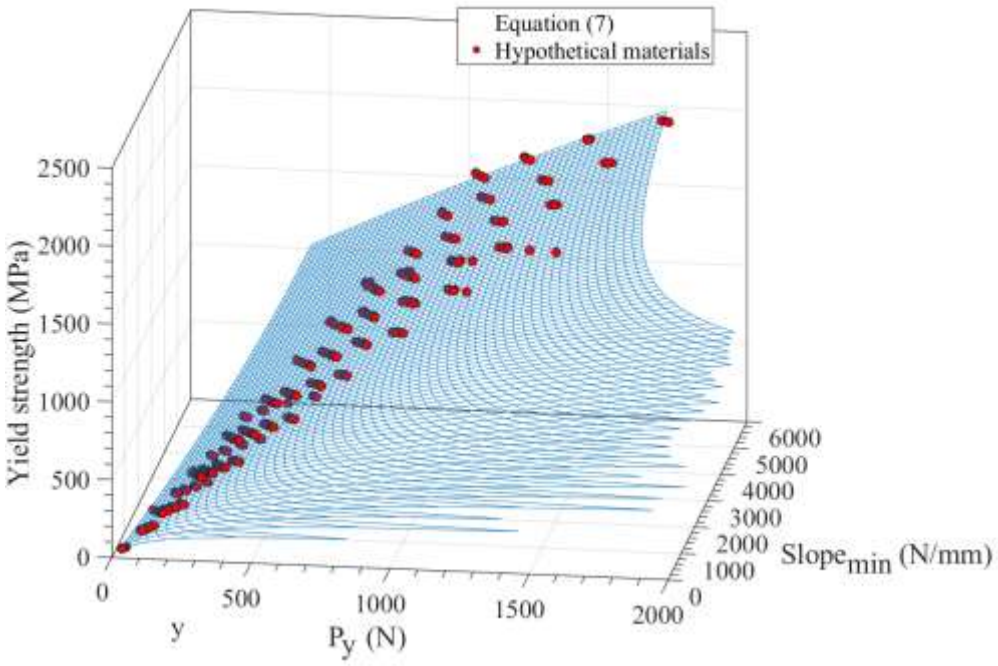

Figure 4. Regression surface of the hypothetical materials with equation (7)

$$\sigma_y = 0.699 \cdot \frac{P_y}{t^2} - 0.258 \cdot \frac{Slope_{min}}{t} \tag{10}$$

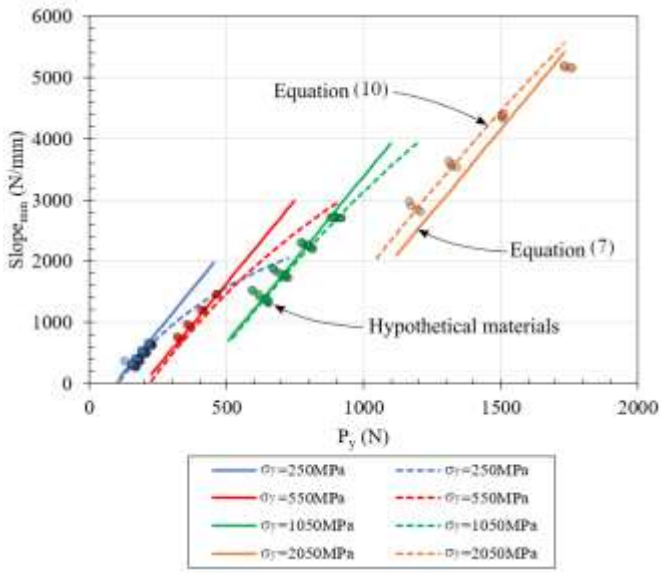

Figure 5. Regression surfaces of the hypothetical materials with equations (7) and (10)

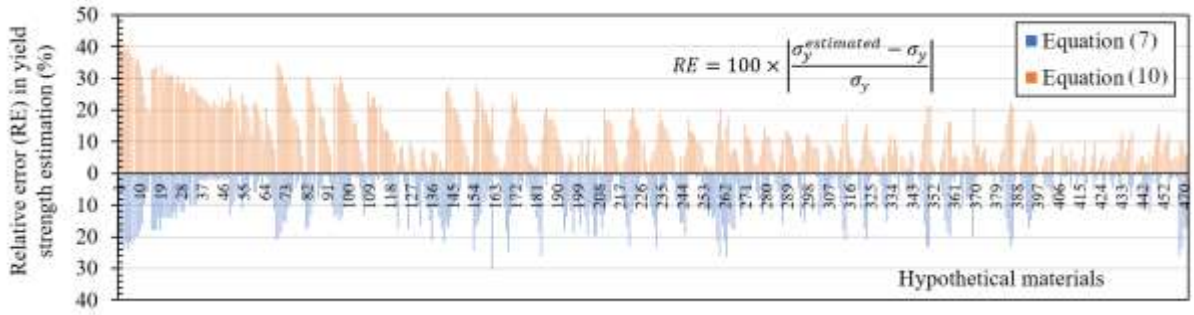

Figure 6. Relative error (RE) in yield strength estimation of the hypothetical materials with equations (7) and (10)

From the systematic FEM analysis performed in the mentioned investigation [22], the correlation equation for the hypothetical materials using the t/10 offset method was calculated (see Figure 7) and is shown in equation (11) with a *NRMSD* = 23.5% (a greater value than the one obtained for the new method *NRMSD* = 15.5%).

$$\sigma_y = 0.336 \cdot \frac{P_y}{t^2} + 24.9 \tag{11}$$

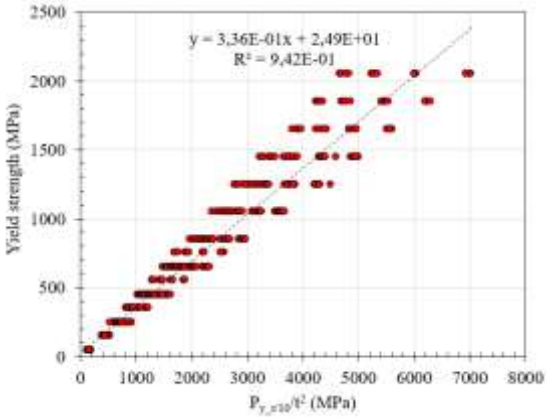

Figure 7. Correlation of the yield strength with the t/10 offset method for the hypothetical materials [22]

5 Experimental tests

Standard tensile tests according to ASTM E8M and SPT's of 16 steel alloys were done. The mechanical properties obtained from the tensile tests are included in Table 1. Figure 8 shows the load-displacement curves obtained from the SPTs. Table 2 shows the parameters extracted from the SPT curves: minimum slope $Slope_{min}$ and yield load P_y of the t/10 offset method.

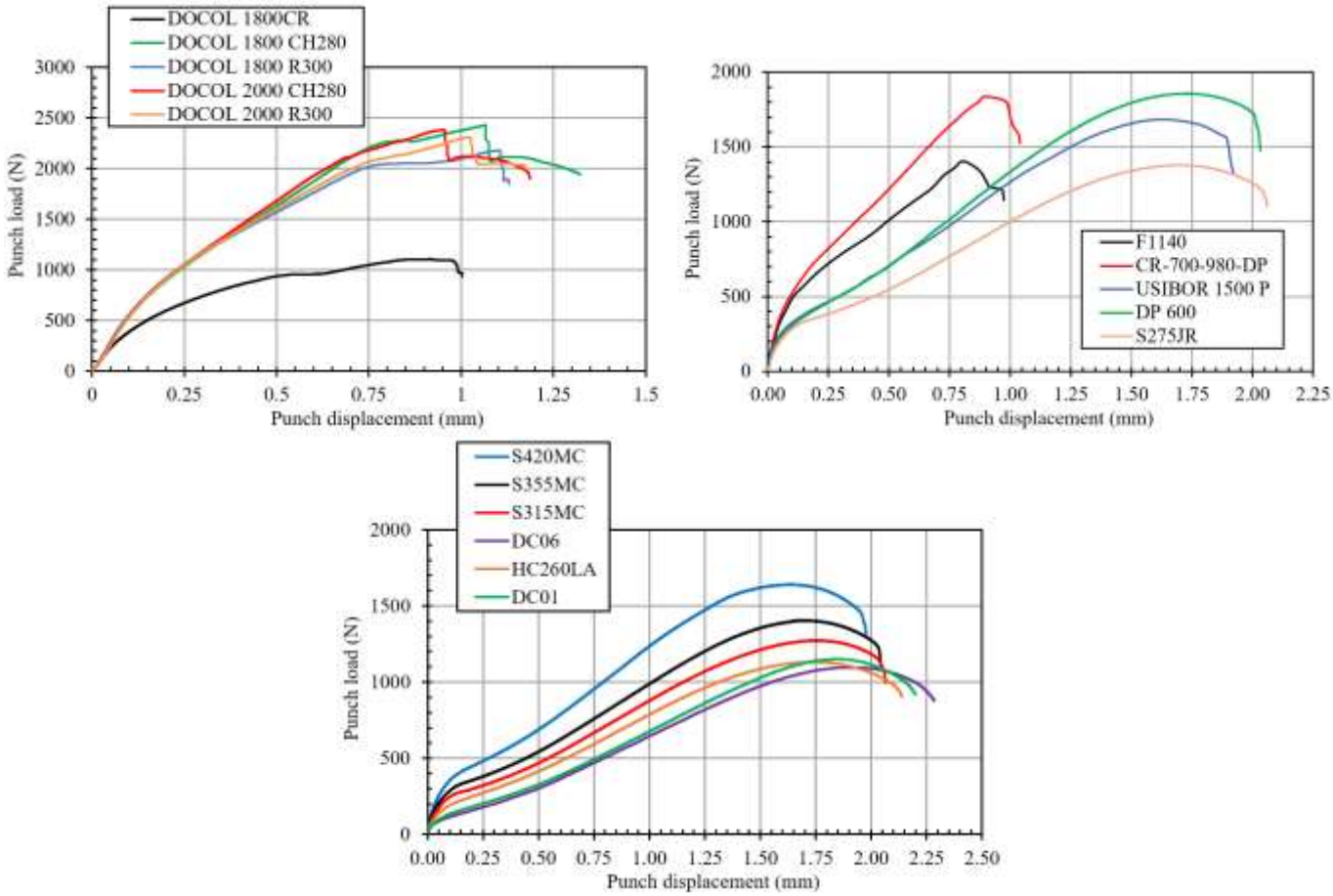

Figure 8. Experimental SPT curves

Material	$Slope_{min}$ (N/mm±%)	$P_{y\,(t/10)}$ (N±%)
DP600	885±1.31	294±0.20
S275JR	567±1.49	267±0.35
HC260LA	514±1.46	179±2.17
DC06	421±3.41	102±1.72
S315MC	488±1.07	228±2.32
S420MC	714±0.50	319±2.33
S355MC	552	263
DC01	439±1.66	126±1.57
F1140	1111±1.38	485±1.05
USIBOR 1500 P	815±0.93	300±1.96
CR-700-980-DP	1515±0.04	525±0.78
DOCOL 1800CR	942	477
DOCOL 1800 CH280	2677	825
DOCOL 1800 R300	2116	841
DOCOL 2000 CH280	2842	887
DOCOL 2000 R300	2278	916

Table 2. SPT parameters of the experimental materials

Figure 9 shows the application of the t/10 offset method to estimate the yield strength of the experimental materials. The obtained regression line (see equation (12)) presented a *NRMSD* = 18.05%. Figure 10 shows the application of the optimized t/10 offset method where the correlation plane was obtained with the Curve Fitting Tool of Matlab. Equation (13) shows the previously mentioned plane with a *NRMSD* = 9.70%, much lower than the deviation value

obtained with the standard t/10 offset method. Figure 11 shows a comparison of the yield strengths estimated with the different correlation methods and the yield strengths obtained from the tensile tests.

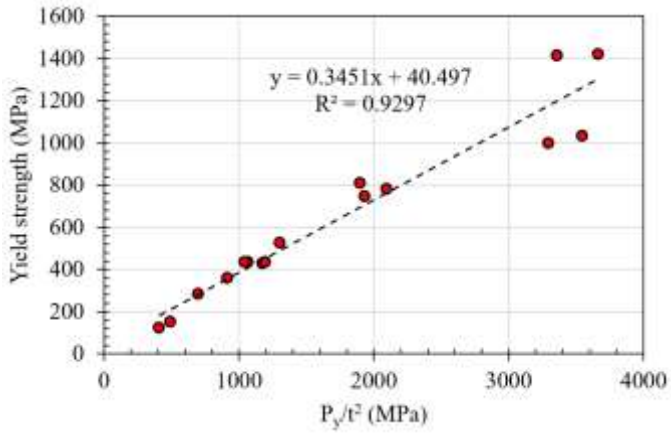

Figure 9. Linear correlation of the t/10 offset method

$$\sigma_y = 0.345 \cdot \frac{P_y}{t^2} + 40.497 \tag{12}$$

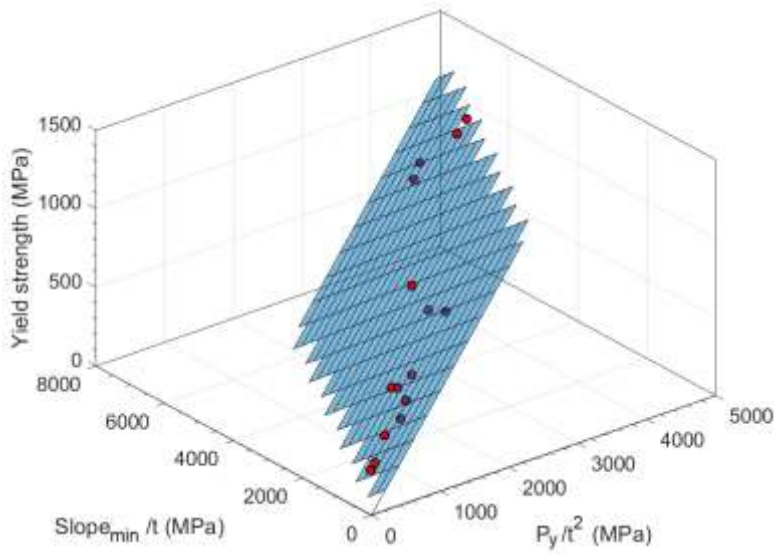

Figure 10. Surface fitting regression with the optimized t/10 offset method

$$\sigma_y = 0.639 \cdot \frac{P_y}{t^2} - 0.202 \cdot \frac{Slope_{min}}{t} \tag{13}$$

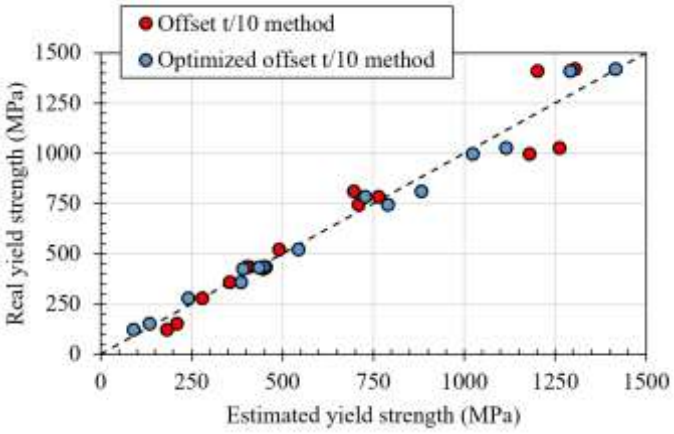

Figure 11. Real vs. estimated yield strengths of the experimental materials

6 Discussion

From previous investigations performed by Calaf-Chica *et al.* [22], a multi-dependency of the correlation methods for the estimation of the yield strength by the SPT with more than one mechanical property was observed. Specifically, the correlation coefficients of the t/10 offset method have shown a dependency with the strain hardening coefficient *n* based on a dependency of the correlation coefficient α_1 (see equation (3)) with the mentioned strain hardening coefficient *n* (see equation (4)). If this multi-dependency is not considered during the application of this correlation method, a significant scattering between the regression line and the experimental data is observed. The analysis performed in this investigation started with the discussion and conclusions obtained in that previous investigation to develop an optimization of the t/10 offset correlation method.

For the experimental tests performed in this study, Table 3 shows their hardening coefficients *n*, calculated with the Kamaya equation (14) [25], and the correlation coefficient α_1, as the relation between the yield strength and the yield load P_y (see equation (15)).

$$n = 3.93\left\{ln\left(\frac{\sigma_u}{\sigma_y}\right)\right\}^{-0.754} \tag{14}$$

$$\alpha_1 = \frac{\sigma_y}{P_y/t^2} \tag{15}$$

Material	n	α_1
DP600	7.8	1.44
S275JR	23.3	1.63
HC260LA	10.1	1.61
DC06	4.6	1.22
S315MC	15.6	1.57
S420MC	18.8	1.60
S355MC	21.9	1.66
DC01	5.5	1.22
F1140	12.6	1.54
USIBOR 1500 P	9.2	1.44
CR-700-980-DP	10.8	1.49
DOCOL 1800CR	22.9	1.69
DOCOL 1800 CH280	6.3	1.21

DOCOL 1800 R300	25.8	1.68
DOCOL 2000 CH280	6.1	1.16
DOCOL 2000 R300	20.8	1.55

Table 3. Hardening coefficients and correlation coefficients for the experimental materials

Figure 12 shows the relation between n and α_1 for the experimental tests performed in this study, and the regression curve obtained with the equation (4). This correlation equation was deduced numerically and relates the correlation coefficient α_1 with the hardening coefficient n. The experimental data corroborate the behavior of the rational equation (4). Thus, the multi-dependency of the yield load P_y of the offset t/10 correlation method with the yield strength and the strain hardening is a proven fact.

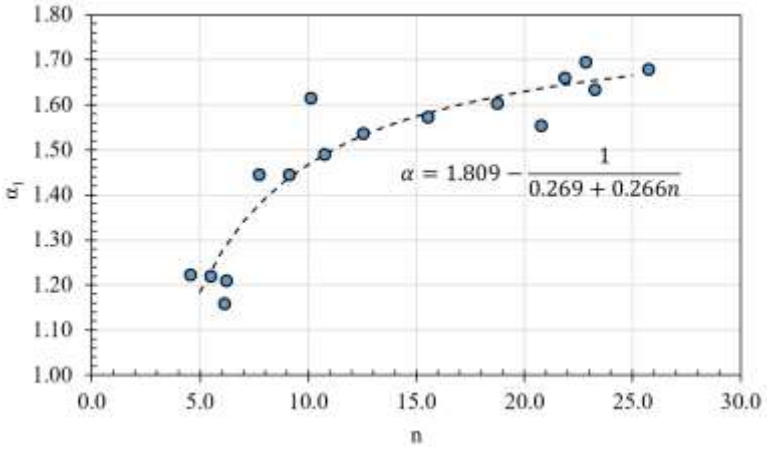

Figure 12. Relation between the hardening coefficient n and the correlation coefficient α_1 for the experimental materials

From the numerical analysis performed in this investigation, the six correlation coefficients A_1 to A_3 and B_1 to B_3 of the multi-dependent equation (7) were calculated in order to substitute the hardening coefficient n of the equation (4) with the minimum slope $Slope_{min}$ of the zone III of the SPT curve. This complex correlation equation could be simplified to the equation of a regression plane because of the hypothetical materials used in that numerical analysis were in a relatively planar zone of the correlation surface. This simplification reduced significantly the number of correlation coefficients from the six parameters of the equation (7) to only two parameters of the equation (10). This novel correlation equation that relates the yield strength with the yield load P_y and the minimum slope $Slope_{min}$ of the zone III of the SPT curve has shown an improvement in the scattering level of the experimental data with the regression surface for a wide selection of steel alloys. Thus, an optimized t/10 offset correlation method has been designed and verified experimentally.

7 Conclusions

This research has given rise to the following conclusions:

(a) The yield strength correlation depends on the yield load P_y obtained with the t/10 offset method and the minimum slope $Slope_{min}$ of the zone III of the SPT curve using complex equations.
(b) For the areas of interest where the most common materials are located, this complex correlation equation may be approximate to plane with acceptable deviation values. This optimized t/10 offset correlation method is represented by the following correlation equation (16):

$$\sigma_y = \alpha_1 \cdot \frac{P_y}{t^2} + \alpha_2 \cdot \frac{Slope_{min}}{t} \tag{16}$$

where α coefficients are obtained with a non-linear least squares regression method.

(c) The correlation coefficients α for the experimental tests performed in this investigation were: α_1 = 0.639, α_2 = -0.202 with a *NRMSD* = 9.70%.

8 Data availability

The raw/processed data required to reproduce these findings cannot be shared at this time as the data also forms part of an ongoing study.

9 References

[1] M.P. Manahan, A.S. Argon, O.K. Harling. Mechanical behavior evaluation using the miniaturized disk bend test, Quaterly Progress Report on Damage Analysis and Fundamental Studies (1981) 82-103. DOE/ER-0046/8.

[2] M.P. Manahan, A.S. Argon, O.K. Harling, The development of a miniaturized disk bend test for the determination of postirradiation mechanical properties, Journal of Nuclear Materials 103 & 104 (1981) 1545-1550.

[3] M.P. Manahan, The development of a miniaturized disk bend test for the determination of post-irradiation mechanical behavior, Doctoral dissertation (1982), Massachusetts Institute of Technology.

[4] J-M. Baik, J. Kameda, O. Buck, Small punch test evaluation of intergranular embrittlement of an alloy steel, Scripta Metallurgica 17 (1983) 1443-1447. DOI: 10.1016/0036-9748(83)90373-3.

[5] J-M. Baik, J. Kameda, O. Buck, Development of small punch tests for ductile-brittle transition temperature measurement of temper embrittled Ni-Cr steels, The use of small-scale specimens for testing irradiated material, ASTM STP888, W.R. Corwin, G.E. Lucas (1986) 92-111.

[6] E. Fleury, J.S. Ha, Small punch tests to estimate the mechanical properties of steels for steam power plant: I. Mechanical strength, International Journal of Pressure Vessels and Piping 75 (1998) 699-706, DOI: 10.1016/S0308-0161(98)00074-X.

[7] J. Calaf-Chica, P. M. Bravo, M. Preciado, Improved correlation for the elastic modulus prediction of metallic materials in the Small Punch Test, International Journal of Mechanical Sciences 134 (2017) 112-122. DOI: 10.1016/j.ijmecsci.2017.10.006

[8] X. Mao, H. Takahashi, Development of a further-miniaturized specimen of 3 mm diameter for TEM disk (Ø 3 mm) small punch tests, Journal of Nuclear Materials 150 (1987) 42-52. DOI: 10.1016/0022-3115(87)90092-4.

[9] A. Okada, M.L. Hamilton, F.A. Garner, Microbulge testing to neutron irradiated materials, Journal of Nuclear Materials 179-181 (1991) 445-448, DOI: 10.1016/0022-3115(91)90120-V.

[10] Y. Ruan, P. Spatig, M. Victoria, Assessment of mechanical properties of the martensitic steel EUROFER97 by means of punch tests, Journal of Nuclear Materials 307-311 (2002) 236-239, DOI: 10.1016/S0022-3115(02)01194-7.

[11] R. Hurst, K. Matocha, Where are we now with the european code of practice for small punch testing?, Proceedings of the International Conference on Small Sample Test Techniques (2012) 4-18.

[12] J. Kameda, O. Buck, Evaluation of the ductile-to-brittle transition temperature shift due to temper embrittlement and neutron irradiation by means of a small-punch test, Materials Science and Engineering 83 (1986) 29-38. DOI: 10.1016/0025-5416(86)90171-0.

[13] M. Bruchhausen, S. Holmström, j.-M. Lapetite, S. Ripplinger, On the determination of the ductile to brittle transition temperature from small punch tests on Grade 91 ferritic-martensitic steel, International Journal of Pressure Vessels and Piping 155 (2017) 27-34. 10.1016/j.ijpvp.2017.06.008

[14] J. Kameda, R. Ranjan, Characterization of deformation and fracture behavior in amorphous and/or ceramic coatings and aluminum alloy substrates by small punch testing and acoustic emission techniques, Materials Science and Engineering A 183 (1994) 121-130, DOI: 10.1016/0921-5093(94)90896-6.

[15] R. Hurst, Y. Li, K. Turba, Determination of fracture toughness from the small punch test using circular notched specimens, Theoretical and Applied Fracture Mechanics 103 (2019) 102238, DOI: 10.1016/j.tafmec.2019.102238.

[16] B. Ule, et al., Small punch test method assessment for the determination of the residual creep life of Service exposed components: outcomes from an interlaboratory exercise, Nuclear Engineering and Design 192 (1999) 1-11, DOI: 10.1016/S0029-5493(99)00039-4.

[17] J.H. Kim, et al., A direct assessment of creep life based on small punch creep test, Theoretical and Applied Fracture Mechanics 104 (2019) 102346, DOI: 10.1016/j.tafmec.2019.102346.

[18] CEN Workshop agreement CWA 15627:2006 E, 2006. "Small Punch Test Method for Metallic Materials." Brussels, CEN.

[19] A. Okada, M.L. Hamilton, F.A. Garner, Microbulge testing to neutron irradiated materials, Journal of Nuclear Materials 179-181 (1991) 445-448, DOI: 10.1016/0022-3115(91)90120-V.

[20] C. Kannan, S. Bhattacharya, D. Sehgal, R. Pandey, Effect of Specimen Thickness and Punch Diameter in Evaluation of Small Punch Test Parameters Toward Characterization of Mechanical Properties of Cr–Mo Steels, Journal of Testing and Evaluation 42 (2014) 1501-1509, DOI: 10.1520/JTE20130299

[21] M.F. Moreno, Effects of thickness specimen on the evaluation of relationship between tensile properties and small punch testing parameters in metallic materials, Materials and Design 157 (2018) 512-522, DOI: 10.1016/j.matdes.2018.07.065

[22] J. Calaf-Chica, P.M. Bravo Díez, M. Preciado Calzada, D. Ballorca-Juez, A systematic FEM analysis of the influence of mechanical properties in the reliability of the correlation methods in the Small Punch Test, International Journal of Mechanical Sciences 153-154 (2019) 299-309, DOI: 10.1016/j.ijmecsci.2019.02.013.

[23] W. Ramberg, W.R. Osgood, Description of stress-strain curves by three parameters, Technical Note 902, NACA, Washington DC, 1943.

[24] J. Calaf-Chica, P.M. Bravo Díez, M. Preciado Calzada, D. Ballorca-Juez, A new correlation method to obtain the ultimate tensile strength with small punch test and its application to hot-stamping processes, AIP Conference Proceedings 2113 (2019) 170012, DOI: 10.1063/1.5112728.

[25] M. Kamaya, Ramberg-Osgood type stress-strain curve estimation using yield and ultimate strengths for failure assessments, International Journal of Pressure Vessels and Piping 137 (2016) 1-12. DOI: 10.1016/j.ijpvp.2015.04.001.